



Facile synthesis and characterization of β -Cd(OH)₂ nanostructures for adsorptive removal of Cr(VI) ions from wastewater: a statistical approach for multivariate sorption optimization

Babar Ali Baig^a, Aydan Elçi^b, Ali Nawaz Siyal^{c,*}, Sanaullah Dehraj^d, Qadeer Khan Panhwar^c, Adnan Ahmed^e, Abdul Rafay Bhatti^a, Fateh Ali^c, Muhammad Yar Khuhawar^c

^aInstitute of Advance Research Studies in Chemical Sciences, University of Sindh, Jamshoro 76080, Pakistan

^bDepartment of Chemistry, University of Ege, Bornova 35040, Turkey

^cInstitute of Chemistry, University of Sindh, Jamshoro 76080, Pakistan, emails: alinsiyal@usindh.edu.pk/
alinawazsiyal@yahoo.com (A.N. Siyal)

^dDepartment of Mathematics and Statistics, Quaid-E-Awam University of Engineering, Science and Technology, Nawab Shah 67480, Pakistan

^eCentre for Environmental Science, University of Sindh, Jamshoro 76080, Pakistan

Received 21 June 2020; Accepted 13 December 2020

ABSTRACT

In the present study, nanostructured β -Cd(OH)₂ adsorbent was synthesized, characterized by Fourier-transform infrared spectroscopy, X-ray diffraction and scanning electron microscopy analysis, and applied for Cr(VI) ions capturing (adsorption) from environmental aqueous samples. The central composite design of 18 adsorption experiments was employed for multivariate sorption optimization. Maximum adsorption (%) of Cr(VI) ions was calculated and found to be 98.5% with relative standard deviation (RSD) \leq 3.5 at optimum concentration 15 mg L⁻¹, pH 4.0, adsorbent dosage 50 mg, shaking time 20 min and shaking speed 120 rpm at 25°C. Langmuir, Freundlich and Dubinin–Radushkevich isotherms fitted well to adsorption data with correlation coefficient (R^2) of 0.993, 0.982 and 0.994, respectively. Mono-layered (Q_m) and multi-layered (K_f) capacities of β -Cd(OH)₂ adsorbent for Cr(VI) ions retention were calculated and found to be 202.02 ± 2.0 and 4.95 ± 2.5 mg g⁻¹, respectively. Sorption energy was calculated and found to be 8.45 ± 2.0 kJ mol⁻¹, indicated chemisorption or ion exchange mechanism for Cr(VI) ions adsorption onto β -Cd(OH)₂ adsorbent.

Keywords: β -Cd(OH)₂ nanostructures; Adsorption; Cr(VI) ions; Equilibrium; Analysis of variance

1. Introduction

Response surface methodology (RSM) was introduced by Box and Wilson [1] for the improvement of the process of manufacturing. The statistical method which solves the multivariate equation using quantitative data obtained from experiments is called RSM [2]. For multivariate optimization, RSM is an effective tool that can be used to

optimize response. It has been widely used for process variables and their interaction affects [3]. RSM has been used for multivariate sorption optimization using central composite design (CCD) [4], Box–Behnken design [5], and Doehlert design (DD) [6]. Among these, the CCD model has been commonly used for sorption optimization with n^k design (k = total number of factors and n = levels of factor). The multivariate sorption optimization by RSM can be performed

* Corresponding author.

in the three steps, designing experiments by n^k formula, estimating the coefficients in a mathematical model, and checking the accuracy and fitting of the proposed model [4].

In chemistry, various methods such as thermogravimetry, electroanalytical, capillary electrophoresis and pre-concentration, adsorption based on co-precipitation, solid-phase extraction, liquid–liquid extraction and cloud point extraction techniques have been optimized by multivariate optimization approach for a decade [7]. The methods can be optimized by univariate and multivariate approaches. In the univariate approach, the optimum response of all independent variables (factors) can be achieved by varying one parameter and keeping other parameters constant. In the multivariate approach, the optimum response of the independent variable (factor) can be achieved by varying two or more factors simultaneously. Usually, in removal studies, the response is removal (%) or sorption capacity and factors are pH, temperature, resin amount, shaking time, shaking speed, and concentration of analyte [4].

The natural ecosystem has been disturbing due to the continued discharging of harmful chemicals (pollutants) into water bodies. Mutagenic and genotoxic chemicals are comparatively more dangerous because they cause heritable disorders, impacting generations [8,9]. Detoxification of contaminated water is becoming a prime task for scientists [10]. Cr(VI) ions exist as CrO_4^{2-} (chromate), $\text{Cr}_2\text{O}_7^{2-}$ (dichromate) or HCrO_4^- (hydrogen chromate) depending on pH [11]. Cr(VI) ion is a longstanding aquatic pollutant, caused by various industrial processes including, electroplating, leather tanning, metal polishing, oxidative dyeing and manufacturing of steel, paints, pigments and textiles [12,13]. Cr(VI) ions can be absorbed by the human body causing health problems. Cr(VI) ions can enter the human body through the skin, mucosa, respiratory tract and digestive tract accumulating in blood, liver and kidney [14]. Cr(VI) ions readily transverse cell membranes through the sulfate transport system as it has structurally similar to sulfate (SO_4^{2-}) and phosphate (PO_4^{3-}). Cr(VI) ions can easily be incorporated into the cell, where it oxidizes biological molecules and causing various health problems. Cr(VI) ion is a strong oxidant, acts as mutagens, teratogens and carcinogens in biological systems [15,16]. US Environmental Protection Agency listed Cr(VI) as the most hazardous toxic pollutant due to its high toxicity and bioaccumulation. US Environmental Protection Agency and World Health Organization fixed 0.1 and 0.05 mg L^{-1} , respectively as the permissible levels of Cr(VI) ions in portable water [17]. Therefore, treatment of Cr(VI) ions containing effluents before discharging to environmental water bodies is strongly recommended. Various methods based on precipitation, electrochemical reduction, ion exchange, solvent extraction, photodegradation, membrane separation and adsorption have been employed for the detoxification of water. Adsorption is comparatively more attractive because of eco-friendly, operational ease, inexpensive, high selectivity, efficiency and recyclability of adsorbents [16].

This study focuses on the facile synthesis and characterization of $\beta\text{-Cd}(\text{OH})_2$ nanostructures for the adsorptive removal of Cr(VI) ions from wastewater. CCD model of RSM will be employed for multivariate sorption optimization.

2. Material and method

2.1. Materials

A flame atomic absorption spectrometer (FAAS) (AAAnalyst 800, USA) was used for Cr(VI) ions determination. Thermo Scientific FT-IR spectrometer (Nicolet iS10, UK) was used for recording Fourier-transform infrared (FT-IR) spectra. Powder X-ray diffraction (XRD) pattern was recorded on diffractometer (Bruker D8 Advance, Germany) by employing $\text{Cu-K}\alpha$ ($\lambda = 1.54056 \text{ \AA}$). Scanning electron microscopy (SEM) images were scanned on a scanning electron microscope (JSM-6490LV, JEOL, Japan). For batch experiments, a shaker (model no. 1-4000, Germany) was used. For pH measurements, a pH meter (InoLab pH 720, Germany) was used. Chemicals (analytical reagent grade) such as $\text{Cd}(\text{NO}_3)_2 \cdot 4\text{H}_2\text{O}$ (99.0%), CH_3COONa (98.5%), NaOH (99.0%), NaH_2PO_4 (99.0%), CH_3COOH (99.5%) and HCl (37.0%) were purchased from Merck (Germany) and used in this work. All the solutions were prepared in double-distilled water. For maintaining the desired pH, $\text{CH}_3\text{COOH}/\text{CH}_3\text{COONa}$, $\text{H}_3\text{PO}_4/\text{NaH}_2\text{PO}_4$ and $\text{NH}_4\text{OH}/\text{NH}_4\text{Cl}$ were used as buffer solutions. STATGRAPHICS version 16.1.11/32 bit (Statpoint Technologies Incorporation, USA) was used for designing.

2.2. Preparation of adsorbent: nanostructured $\beta\text{-Cd}(\text{OH})_2$

Nanostructured $\beta\text{-Cd}(\text{OH})_2$ was synthesized following the procedure [18] as aqueous solutions A: 4.0 mol L^{-1} NaOH and B: 2.0 mol L^{-1} $\text{Cd}(\text{NO}_3)_2 \cdot 4\text{H}_2\text{O}$ were prepared. Solution A was added dropwise into 250 mL of B with stirring magnetically. A was added continuously until the pH of the reaction mixture was reached to 10, and heated at 50°C for 5.0 h. The mixture was settled at room temperature and filtered. The precipitated product was subsequently washed with water and ethanol and oven-dried at 40°C.

2.3. Factors and CCD model

Factors are independent variables such as, A: adsorbent dose, B: initial concentration of adsorbate, C: pH of solution and D: shaking time. Response (removal) changes with change in factors. In the CCD model, factors were fixed at minimum (−1), maximum (+1) and intermediate (0) levels (Table 1) for multivariate sorption optimization [4]. CCD model with n^k design, where $k = 4$ (number of independent variables and $n = 2$ (levels of variables: minimum and maximum)) formulated 16 adsorption experiments with two replicates (Table 2). Hypothetically, the adsorption (%) of Cr(VI) ions for 18 experiments were predicted by

Table 1
Factors and their levels for CCD model

Factors	−1	0	+1
A: adsorbent dose (mg)	10.0	55.0	100.0
B: concentration (mg L^{-1})	5.0	15.0	25.0
C: pH	2.0	5.5	9.0
D: shaking time (min)	10.0	95.0	180.0

the CCD model. The 18 adsorption experiments for Cr(VI) ions retention onto nanostructured β -Cd(OH)₂ adsorbent were performed in the laboratory, results (Table 2) revealed that experimental and predicted removals were found good in agreement with R^2 of 99.97%, which indicated well-fitting of CCD model to adsorption experiments.

2.4. Adsorption experiment

The optimum factors for adsorption of Cr(VI) on β -Cd(OH)₂ adsorbent was predicted by the CCD model as

Table 2
Design and experiments

Run	A	B	C	D	Removal (%)		
					Observed	Predicted	Residual
1	1	1	-1	1	92.8	92.9	7.2
2	0	1	0	0	88.3	88.2	11.7
3	1	1	1	-1	93.6	94.0	6.4
4	-1	1	-1	-1	93.5	93.5	6.5
5	-1	0	0	0	99.9	99.9	0.1
6	-1	-1	-1	-1	94.2	94.1	5.8
7	-1	1	1	1	85.9	86.1	14.1
8	0	0	-1	0	89.7	89.7	10.3
9	0	-1	0	0	97.3	97.2	2.7
10	1	-1	-1	1	95.5	95.6	4.5
11	1	-1	1	-1	98.5	98.4	1.5
12	0	0	0	1	84.4	84.3	15.6
13	-1	-1	1	1	96.1	95.7	3.9
14	0	0	0	-1	99.3	99.5	0.7
15	0	0	1	0	88.8	88.7	11.2
16	1	0	0	0	96.3	96.2	3.7
17	0	0	0	0	90.8	90.7	9.2
18	0	0	0	0	89.9	90.3	10.1

50 mg of Cd(OH)₂ adsorbent was placed into a 25 mL bottle, containing 10 mL of 15 mg L⁻¹ Cr(VI) ions of pH 4.0 and shaken at 120 rpm for 20 min at 25°C. The mixture was filtered and filtrate was subjected to FAAS for determination of residual Cr(VI) ions. The adsorption (%) of Cr(VI) ions was calculated by Eq. (1) and found to be 98.5% with RSD \leq 3.5.

$$\text{Adsorption (\%)} = \frac{(C_i - C_f)}{C_i} \times 100 \quad (1)$$

where C_i and C_f are the initial and final concentrations of Cr(VI) ions, respectively.

3. Results and discussions

3.1. Characterization

3.1.1. FT-IR spectroscopy

FT-IR spectrum (Fig. 1) of as-synthesized β -Cd(OH)₂ shows stretching vibrations at 3,600.85 and 3,333.86 cm⁻¹ correspond to O–H bonds of β -Cd(OH)₂ and water, respectively [19], bending vibration at 1,645.97 cm⁻¹ corresponds to O–H bond of water [20], and stretching vibration at 857.26 cm⁻¹ attributed to Cd–O bond of β -Cd(OH)₂, which confirmed the formation of β -Cd(OH)₂ [21].

3.1.2. X-ray diffraction

Powder XRD pattern (Fig. 2) of nanostructured β -Cd(OH)₂ shows diffraction peaks at 2θ values 19.09°, 29.75°, 35.49°, 38.43°, 49.23°, 52.51°, 56.33°, 61.46°, 64.87°, 67.06°, 67.39° and 74.74° correspond to (001), (100), (101), (002), (102), (110), (111), (200), (201), (112), (103) and (202) planes (hkl) of hexagonal crystal system of β -Cd(OH)₂, respectively, which confirmed the formation of hexagonal crystal system of β -Cd(OH)₂ [18,22]. According to Bragg's law ($d = n\lambda/2\sin\theta$, where λ is the wavelength of X-ray

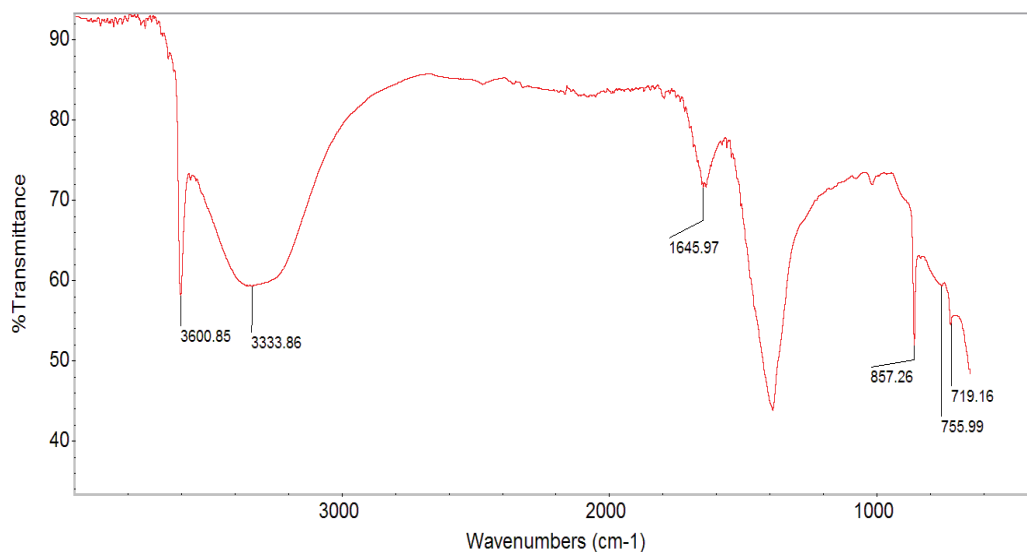


Fig. 1. FT-IR spectrum of as-synthesized nanostructured β -Cd(OH)₂.

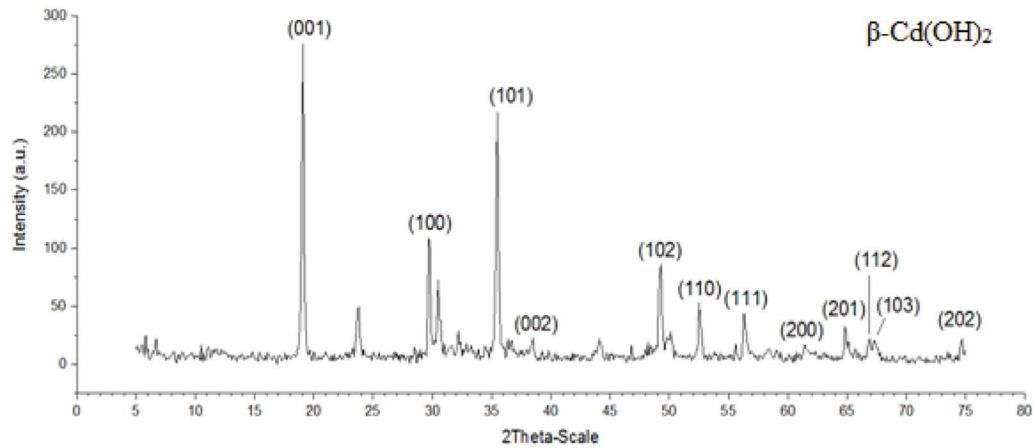


Fig. 2. XRD pattern of as-synthesized nanostructured β -Cd(OH)₂.

(for Cu-K α , $\lambda = 1.54056 \text{ \AA}$) and $n = 1$ (order of diffraction) and θ is Bragg's angle in radian [21], the d -spacings (d_{hkl}) of hexagonal crystal system of β -Cd(OH)₂ were calculated (Table 3) and lattice parameters such as a and c were found to be 3.46 and 4.60 \AA using (001) and (100) planes, respectively. Using Scherrer equation ($D = K\lambda/\beta\cos\theta$, where D = crystalline diameter (nm), λ is the wavelength (nm) of X-ray (for Cu-K α , $\lambda = 1.54056 \text{ \AA}$), K is Scherrer's constant ($K = 0.9$) and θ is Bragg's angle in radian, β is the full-width at half-maximum of planes in radian [23], the average crystallite size of β -Cd(OH)₂ was calculated and found to be 166.68 nm (Table 3). The SEM image (Fig. 3) of β -Cd(OH)₂ revealed the successful construction of nano-sized material.

3.2. Multivariate sorption optimization

3.2.1. Effect of concentration and pH

Effect of factors such as, concentration 5–25 mg L⁻¹ and pH 1–10 on the removal (%) of Cr(VI) ions at optimum

adsorbent dosage 50 mg and contact time 20 min was examined. Plot (Fig. 4) depicts that the retention was slightly decreased 100%–95% with increasing of the concentration 5–20 mg L⁻¹ at any pH. The removal was significantly decreased with further increasing of concentration 20–25 mg L⁻¹ due to the saturation at the surface of the adsorbent.

3.2.2. Effect of adsorbent dosage and pH

Fig. 5 depicts the effect of two factors such as, adsorbent dosage 10–100 mg and pH 1–10 on Cr(VI) ions adsorption at concentration 15 mg L⁻¹ and agitating time 20 min was examined. The plot shows that removal was decreased significantly with increasing of pH of sorbent as nanostructured β -Cd(OH)₂ became least active for retention of Cr(VI) ions at higher pH. At pH 1–4, nanostructured β -Cd(OH)₂ worked well for removal (>95%) of Cr(VI) ions.

Table 3
XRD parameters of as synthesized nanostructured β -Cd(OH)₂

2 θ	hkl	Full-width half-maximum	Crystallite size (nm)	Lattice strain (nm)	d -spacing (nm)
19.09	001	0.436	19.31	0.0113	0.46
29.75	100	0.470	18.27	0.0077	0.30
35.49	101	0.439	19.85	0.0060	0.25
38.43	002	0.194	45.31	0.0024	0.23
49.23	102	0.462	19.76	0.0044	0.18
52.51	110	0.347	26.67	0.0031	0.17
56.33	111	0.339	27.77	0.0028	0.16
61.46	200	0.006	1,609.31	0.0000	0.15
64.87	201	0.099	99.33	0.0007	0.14
67.06	112	0.624	15.96	0.0041	0.14
67.39	103	0.135	73.89	0.0009	0.14
74.78	202	0.422	24.75	0.0024	0.13
Average crystallite size (nm)			166.68		

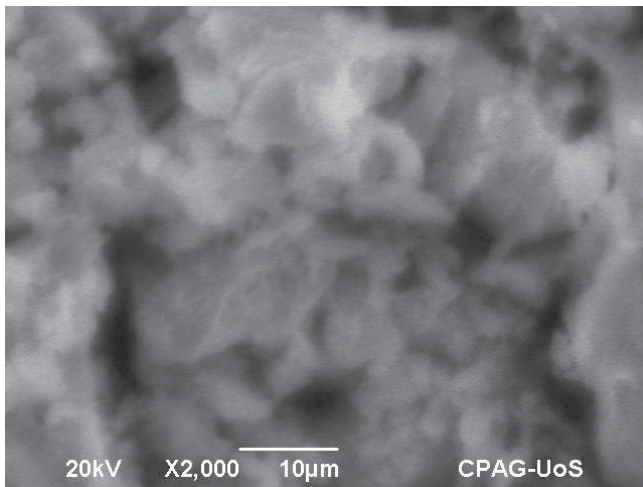


Fig. 3. SEM image of as-synthesized nanostructured β -Cd(OH)₂.

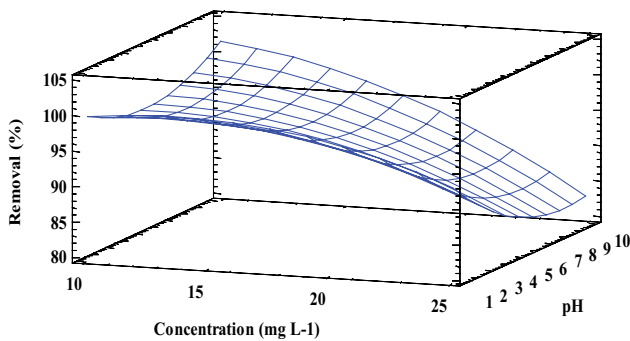


Fig. 4. Effect of concentration and pH on Cr(VI) ions adsorption.

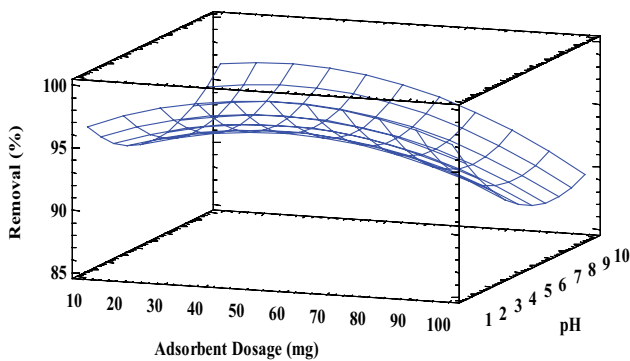


Fig. 5. Effect of adsorbent dosage and pH on Cr(VI) ions adsorption.

3.2.3. Effect of adsorbent dosage and shaking time

Effect of two factors such as, dosage 10–100 mg and shaking time 10–180 min on the removal (%) of Cr(VI) ions at concentration 15 mg L⁻¹ and pH 4.0 was examined. The plot (Fig. 6) depicts that adsorption was significantly enhanced by increasing shaking time at any dose of the adsorbent. The adsorbent dosage of 50 mg worked well for removal (>95%) of Cr(VI) ions.

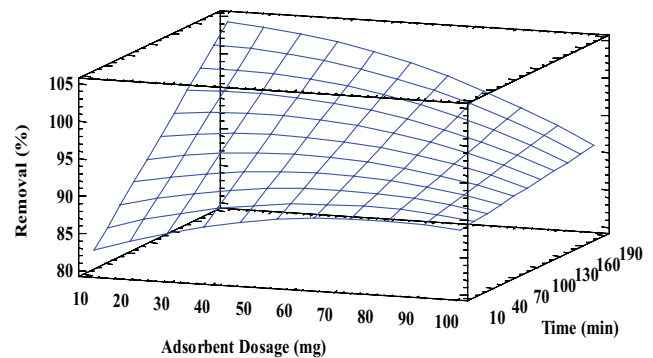


Fig. 6. Effect of adsorbent dosage and shaking time on Cr(VI) ions adsorption.

3.2.4. Effect of concentration and shaking time

Effect of two factors such as, concentration 5–25 mg L⁻¹ and shaking time 10–180 min on of Cr(VI) ions retention at pH 4.0 and adsorbent dosage 50 mg was examined. The plot (Fig. 7) shows that adsorption was declined with increasing concentration, and the extent of the decline was increased with increasing shaking time. The adsorption was enhanced by increasing agitating time.

3.2.5. Effect of pH and shaking time

Effect of two factors such as, adsorbent dosage 10–100 mg and pH 2–9 on Cr(VI) ions adsorption at concentration 15 mg L⁻¹ and dosage 50 mg was examined. The plot (Fig. 8) shows that at shaking time 10–100 min, the removal was decreased with increasing of pH 1–6, remained almost unchanged at pH 6–7 and slightly increased at pH 7–10.

3.2.6. Effect of adsorbent dosage and concentration

Effect of two factors such as, adsorbent dosage 10–100 mg and concentration 5–25 mg L⁻¹ on the response at pH 5 and shaking time 20 min was examined. The plot (Fig. 9) shows that the removal was declined with increasing of adsorbent dosage at lower concentration levels and slightly increased at higher concentration levels. Similarly, the removal was decreased with increasing of concentration at adsorbent dosages of 10–50 mg and slightly changed at adsorbent dosages of 50–100 mg.

3.3. Effect of factors

The individual effects (Fig. 10) of the factors were predicted by statistical analysis. Trends show that three factors (adsorbent dosage, concentration and shaking time) have the almost same effect as removal (%) was enhanced by increasing of the factors and then decreased with further increasing of the factors (adsorbent dosage, concentration and shaking time), while a significant decrease in removal (%) was achieved with increasing of pH. The effect of pH can be justified as the adsorbent was positively charged due to the protonation in an acidic medium. The Cr(VI) species possessing a negative charge

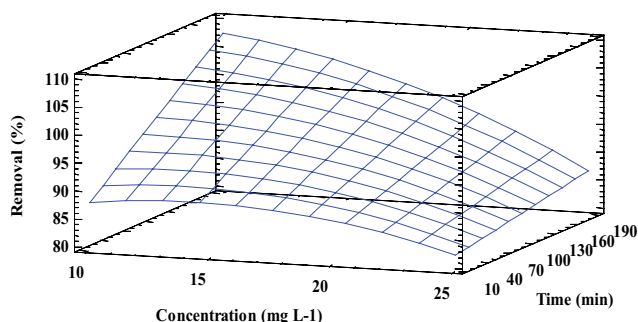


Fig. 7. Effect of concentration and shaking time on Cr(VI) ions adsorption.

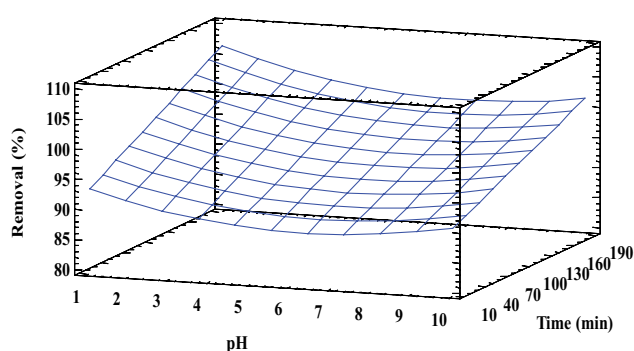


Fig. 8. Effect of pH and shaking time on Cr(VI) ions adsorption.

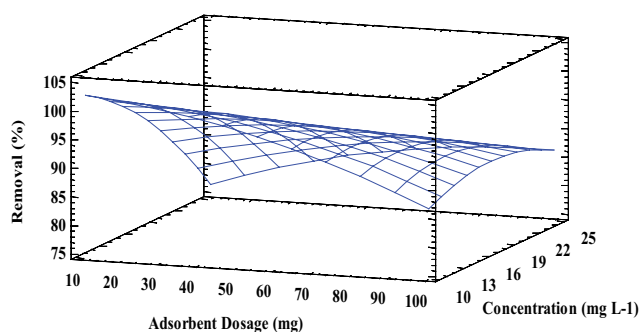


Fig. 9. Effect of adsorbent dosage and concentration on Cr(VI) ions adsorption.

which adsorbed predominantly onto the positively charged adsorbent. In an alkaline medium, the adsorbent became negatively charged due to the deprotonation, which prevented the adsorption of negatively charged Cr(VI) ion species [11].

3.4. Analysis of variance

Analysis of variance (ANOVA) (Table 4) with four factors (three levels) evaluated the significance of factors and fitting of the CCD model. The model was fitted well to the data as $P \leq 0.05$ and a higher value of F for all interactions except DD (P : 0.9260 and F : 0.0100), which

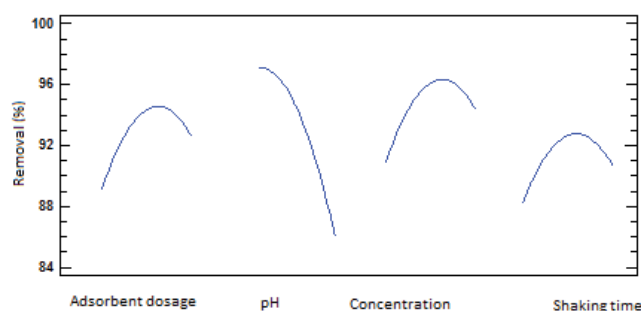


Fig. 10. Effects of four factors on Cr(VI) ions adsorption.

indicated all null hypotheses were rejected except DD [24,25]. The sum of squares (SS) is the measure of scattering of experimental data from the mean of replicated runs. Statistically, SS can be used to find the function that best fits the data. The SS was calculated by Eq. (2) for each of the replicates ($n = 2$). Mathematically, the term mean square (MS) was obtained by dividing SS by degrees of freedom ($n-1$) as calculated by Eq. (3).

$$SS = \sum_{i=0}^n (X_i - \text{Mean})^2 \quad (2)$$

$$MS = \frac{SS}{(n-1)} \quad (3)$$

where X_i is output (response) of individual replicates of the run, and $(X_i - \text{mean})$ is the deviation of response from the mean of responses of replicates. R -squared (R^2) measures the proportion of the variation in response (removal) against the factors (independent variables) in the CCD model. It assumes that all factors participate in varying the response. R^2 can be obtained by dividing the sum of squares of residuals (SS_r) by the total sum of squares (SS_T) as calculated by Eq. (4). The R^2 statistic indicated the well-fitting of the CCD model and explained 99.88% of the variability in removal with the factors.

$$R^2 = \left(1 - \frac{SS_r}{SS_T} \right) \times 100 \quad (4)$$

3.5. Effect of matrix ions

Effect matrix ions on the adsorption of Cr(VI) ions onto nanostructured β -Cd(OH)₂ adsorbent was examined. Thus, the adsorbent worked well for the retention of Cr(VI) ions in presence of various ions. Therefore, nanostructured β -Cd(OH)₂ adsorbent possessed high tolerance limit for studied ions as shown in Table 5.

3.6. Equilibrium studies

Adsorption equilibrium experiments were carried out by varying the initial concentration of Cr(VI) ions in the range of 2.5–50 mg L⁻¹, and keeping optimum levels adsorbent dosage 50 mg, pH 4.0, shaking time 20 min at 25°C.

Table 4
Analysis of variance

Factors	Mean squares	DF	Sum of squares	F-ratio	P-value
A: adsorbent dosage	5.24912	1	5.24912	31.050	0.0121
B: concentration	82.9214	1	82.9214	490.56	0.0001
C: pH	36.4517	1	36.4517	215.65	0.0014
D: shaking time	68.5322	1	68.5322	405.44	0.0010
AA	19.1086	1	19.1086	113.05	0.0070
AB	66.1468	1	66.1468	391.33	0.0001
AC	27.5075	1	27.5075	162.73	0.0211
AD	33.0448	1	33.0448	195.49	0.0007
BB	27.2210	1	27.221	161.04	0.0011
BC	69.8505	1	69.8505	413.24	0.0003
BD	20.4151	1	20.4151	120.78	0.0016
CC	32.3745	1	32.3745	191.53	0.0019
CD	2.32118	1	2.32118	13.730	0.0341
DD	0.00172	1	0.00172	0.0100	0.9260
Total error	0.16903	3	0.50709	–	–
Total (corr.)	431.971	17	–	–	–

R-squared = 99.88%; R-squared (adjusted for DF) = 99.33%; standard error of estimate = 0.41; mean absolute error = 0.119.
DF: degree of freedom.

Table 5
Adsorption of Cr(VI) ions: effect of matrix ions

Interfering ions	Salts added	Concentration (mg L ⁻¹)	Removal (%) ± RSD
Na ⁺ , K ⁺ , Mg ²⁺ , Ca ²⁺	Chloride salts	500	≥91.2 ± ≤4.0
Zn(II), Pb(II), Cu(II), Cd(II), Co(II)	Nitrate salts	50	≥95.2 ± ≤3.5
Cl ⁻ , F ⁻ , HCO ₃ ⁻ , CO ₃ ²⁻ , SO ₄ ²⁻ , NO ₃ ⁻ , CH ₃ COO ⁻	Sodium salts	200	≥89.7 ± ≤3.5

RSD: Relative standard deviation.

Langmuir, Dubinin–Radushkevich (D–R), and Freundlich isotherms were plotted for analyzing the adsorption data.

3.6.1. Langmuir isotherm

Based on assumptions that adsorbent possesses structurally identical active sites which are homogeneously distributed and energetically equivalent. Adsorption takes place at the active sites onto the adsorbent without interaction between adsorbate molecules or ions. Mathematically, the Langmuir isotherm model (linear form) and R_L (separation factor) are represented by Eqs. (5) and (6), respectively [26].

$$\frac{C_e}{C_{ads}} = \frac{1}{Q_m} C_e + \frac{1}{Q_m b_L} \quad (5)$$

$$R_L = \frac{1}{1 + (b_L C_i)} \quad (6)$$

where C_i : initial concentration (mg L⁻¹) of Cr(VI) ions in the aqueous phase, C_e : concentration (mg L⁻¹) of Cr(VI) ions

in aqueous at equilibrium stage, C_{ads} : amount of Cr(VI) ions (mg) adsorbed onto 1 g of adsorbent at equilibrium stage. Q_m : mono-layered sorption capacity (mg g⁻¹) and b_L is Langmuir constant (L mg⁻¹), which is related to the binding energy of adsorbate and the affinity of active sites for adsorbate. The Langmuir isotherm (C_e/C_{ads} vs. C_e) was plotted (Fig. 11) and fitted well to the experimental data with R^2 of 0.993. The Q_m for Cr(VI) ions was calculated and found to be 202.02 ± 2.0 mg g⁻¹. R_L values were calculated and found in the range of 0.027–0.881, which indicated that adsorption of Cr(VI) ions was favorable as $0 < R_L < 1$ [27].

3.6.2. Freundlich isotherm

Based on assumptions that adsorbent is heterogeneous which possesses structurally and energetically unequal active sites, possessing unlike affinity for adsorbate with different adsorption energy. Multi-layered adsorption takes place onto the adsorbent by interacting with adsorbate to active sites and adsorbate to adsorbate. Mathematically, Freundlich isotherm (linear form) is represented by Eq. (7) [28].

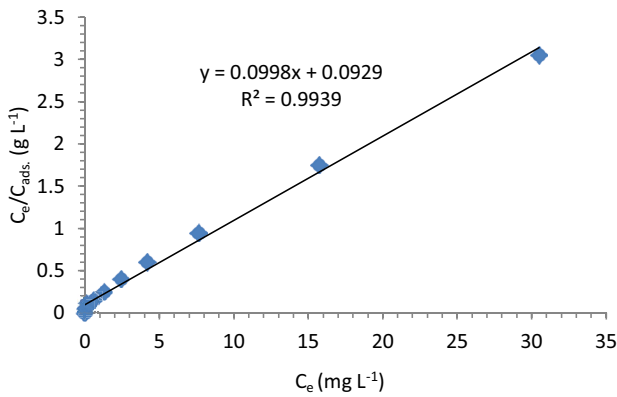


Fig. 11. Langmuir isotherm: Cr(VI) ions adsorption onto nanostructured β -Cd(OH)₂.

$$\log C_{ads} = \frac{1}{n_f} \log C_e + \log K_f \quad (7)$$

where K_f (mg g^{-1}) and n_f (L mg^{-1}) are Freundlich constants, related to capacity (multi-layered) and adsorption favorability, respectively. The adsorption may be poor ($n < 1$), moderate ($n = 1-2$) and good ($n = 2-10$) [28]. Freundlich isotherm ($\log C_{ads}$ vs. $\log C_e$) was plotted (Fig. 12) and fitted well to the data with R^2 of 0.982. K_f for Cr(VI) ions was calculated and found to be $4.95 \pm 2.5 \text{ mg g}^{-1}$ with n value of 4.65, suggested good adsorption onto the active sites, heterogeneously distributed onto the surface of the adsorbent.

3.6.3. Redlich–Peterson isotherm

This isotherm is a three-parameter based adsorption model, including the parameters of Langmuir and Freundlich isotherms models. The Redlich–Peterson (R–P) isotherm is considered as an accurate isotherm to determine the best fitting of either Langmuir or Freundlich isotherms [29]. The non-linear form of R–P isotherm (Eq. (8)) was plotted (Fig. 13) and all three constant values were determined by Microsoft Excel Add-In solver.

$$C_{ads} = \frac{AC_e}{1 + BC_e^\beta} \quad (8)$$

where A (L g^{-1}) and B (L mg^{-1}) are R–P isotherm constants, were calculated and found to be 20.11 and 3.24, respectively, and β is exponent, that can be in the range of 0–1. The value of β was calculated and found to be 0.85, indicating that data is following more Langmuir than Freundlich isotherm and the value of β is near to the unity [30].

3.6.4. Dubinin–Radushkevich isotherm

Based on assumptions that the adsorbent’s surface is not heterogeneous and possessing porosity. D–R isotherm estimates the porosity of the adsorbent and sorption energy. Mathematically, D–R isotherm (linear form) is represented by Eq. (9) [26,28].

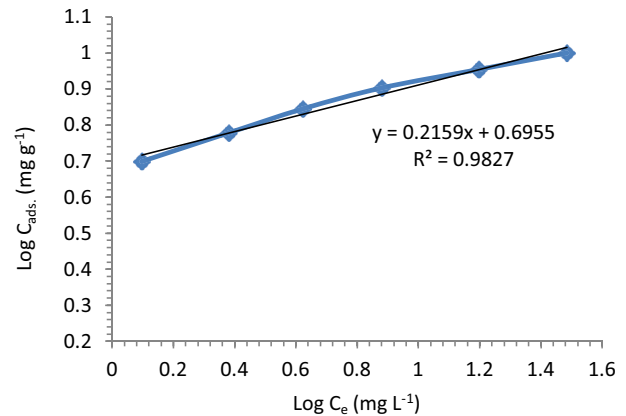


Fig. 12. Freundlich isotherm: Cr(VI) ions adsorption onto nanostructured β -Cd(OH)₂.

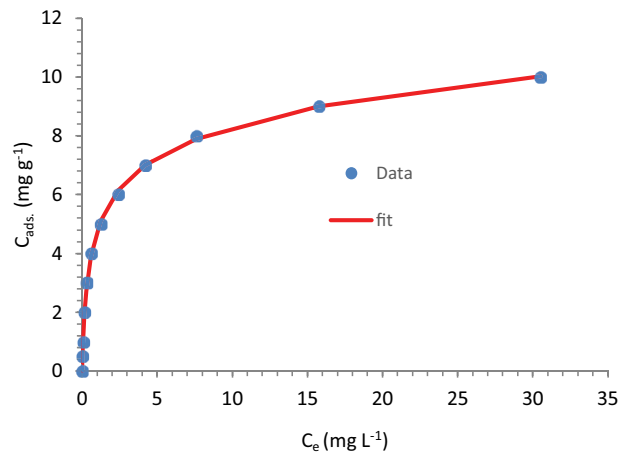


Fig. 13. Redlich–Peterson isotherm: Cr(VI) ions adsorption onto nanostructured β -Cd(OH)₂.

$$\ln C_{ads} = \ln K_{D-R} - \beta \epsilon^2 \quad (9)$$

where K_{D-R} : total sorption capacity (mg g^{-1}), β : activity coefficient, related to the slope of D–R isotherm plot and ϵ is Polanyi potential, calculated by Eq. (10).

$$\epsilon = RT \ln \left(1 + \frac{1}{C_e} \right) \quad (10)$$

where R : general gas constant = $8.314 \text{ J mol}^{-1} \text{ K}^{-1}$, T : temperature in Kelvin = 298 K and E is sorption energy, can be calculated by Eq. (11).

$$E = \frac{1}{\sqrt{-2\beta}} \quad (11)$$

D–R isotherm ($\ln C_{ads}$ vs. ϵ^2) was plotted (Fig. 14) and fitted well with R^2 of 0.994. The total sorption capacity (K_{D-R}) was calculated from intercept (-1.663) of the plot

and found to $9.86 \pm 2.5 \text{ mg g}^{-1}$. The E was calculated from the slope of the plot and found to $8.45 \pm 2.0 \text{ kJ mol}^{-1}$, indicated adsorption of Cr(VI) ions proceeded via chemisorption or ion exchange as E is $8\text{--}16 \text{ kJ mol}^{-1}$ [27].

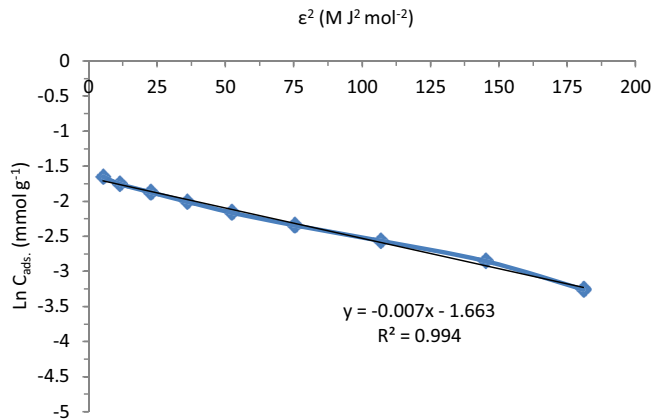


Fig. 14. Dubinin–Radushkevich isotherm: Cr(VI) ions adsorption onto nanostructured $\beta\text{-Cd}(\text{OH})_2$.

3.7. Comparative capacities

Different adsorbents have been reported for adsorptive removal of Cr(VI) ions. As synthesized nanostructured $\beta\text{-Cd}(\text{OH})_2$ possesses a comparatively high capacity for Cr(VI) ions uptake as shown in Table 6.

3.8. Application of the method

The water samples were spiked by standard addition. All the samples were subjected to the removal of Cr(VI) ions according to the developed method. Removals (%) of Cr(VI) ions from water samples were calculated by Eq. (2) and found to be ≥ 86.4 with RSD $\leq 5.5\%$ (Table 7).

4. Conclusion

Nanostructured $\beta\text{-Cd}(\text{OH})_2$ adsorbent was crystalline in nature with an average crystallite size of 166.68 nm. The synthesized material is novel and worked well for the adsorption of Cr(VI) ions from wastewater samples. The method is comparatively more attractive because of its eco-friendly, operational ease, inexpensive, high

Table 6
Capacities of different adsorbents for adsorption of Cr(VI) ions

Adsorbents	pH	Q (mg g^{-1})	K_f (mg g^{-1})	References
MgAl mixed hydroxides	4.0	109.6	45.76	[31]
MgAl- CO_3 LDH	6.0	–	17.0	[32]
NiMgAl- SO_4 LDH	–	103.4	67.7	[33]
NiMgAl- SO_4 LDH	–	49.6	4.9	[33]
NiFe- NO_3 LDH	–	26.8	–	[34]
MgAl- CO_3 LDH	12	339.0	13.3	[35]
NiAl- NO_3 LDH	2.0	34.1	–	[36]
ZnAl-Cl LDH	5.0	172.4	76.2	[37]
MgAl- NO_3 LDH	6.5	30.3	1.4	[38]
NiAl- NO_3 LDH	6.5	57.5	2.0	[38]
ZnAl- NO_3 LDH	6.5	68.1	1.7	[38]
CoFe- CO_3 LDH	7.5	27.6	–	[39]
MgAl-Cl LDH	6.0	58.8	33.3	[40]
MgAl- NO_3 LDH	6.0	71.9	18.4	[40]
MgAl- SO_4 LDH	6.0	55.6	0.4	[40]
NiAl-Cl LDH	–	104.0	–	[41]
CoAl-Cl LDH	–	98.8	–	[41]
CoAl- NO_3 LDH	2.0	109.5	8.61	[42]
CoAl- NO_3 LDH/Bentonite	2.0	211.9	4.4	[42]
MgAl- NO_3 LDH/Graphene	–	172.6	183.8	[43]
ZnAl- NO_3 LDH/ NiFe_2O_4 /EDTA	6.0	66.1	21.4	[44]
MgAl- NO_3 LDH/ CoFe_2O_4	2.0	72.4	6.76	[45]
MgAl- NO_3 LDH/L-Arginine	8.0	84.2	–	[46]
CoAl- NO_3 LDH/L-Arginine	8.0	77.8	–	[46]
ZnAl- NO_3 LDH/L-Arginine	8.0	55.9	–	[46]
MgAl- NO_3 LDH/Polyaniline	3.0	435.0	–	[47]
$\beta\text{-Cd}(\text{OH})_2$ nanostructures	4.0	202.02 ± 2.0	4.95 ± 2.5	This work

LDH – layered double hydroxide; EDTA – ethylenediaminetetraacetic acid.

Table 7
Spiked wastewater samples: removal of Cr(VI) ions

Samples	Added (mg L ⁻¹)	Found (mg L ⁻¹)	Removal (%) ± RSD
S-I	0.0	ND	–
	5.0	4.8	96.0 ± 3.5
	10	9.6	96.0 ± 2.5
	20	19.0	95.0 ± 4.0
	25	23.2	92.8 ± 2.5
S-II	0.0	ND	–
	5.0	4.7	94.0 ± 3.5
	10	9.4	94.0 ± 4.0
	20	18.5	92.5 ± 3.0
	25	23	92.0 ± 4.0
S-III	0.0	ND	–
	5.0	4.5	90.0 ± 2.5
	10	9.2	92.0 ± 4.0
	20	17.3	86.5 ± 3.5
	25	22.1	88.4 ± 4.0

S-I: Bottled water (Nestle, purchased from local market in Jamshoro, Pakistan); S-II: water sample collected from hand-pump in Sehwan Sharif, Sindh, Pakistan; S-III: wastewater sample collection from the combined effluent treatment plant in Korangi, Karachi, Pakistan.

ND: Not detected; RSD: Relative standard deviation.

selectivity, efficiency and recyclability of the adsorbent. CCD model of 18 experiments employed for multivariate sorption optimization. ANOVA suggested that the CCD model was fitted well to the experimental data as $P \leq 0.05$ and higher value of F for all interactions except DD (P : 0.9260 and F : 0.0100), indicating null hypotheses were rejected except DD interaction. Individually, three factors (adsorbent dosage, concentration and shaking time) have almost the same effect as removal (%) was increased with increasing of the factors and then decreased with further increasing of the factors, while a significant decrease in removal (%) was observed with increasing of pH. Equilibrium study suggested monolayered and multi-layered adsorption with sorption energy of 8.45 ± 2.0 kJ mol⁻¹. The non-linear form of R–P isotherm was plotted. The value of β was calculated and found to be 0.85, indicating that data is following more Langmuir than Freundlich isotherm and the value of β is near to the unity. The Cr(VI) species possessing a negative charge which adsorbed predominantly onto the positively charged adsorbent. The material can be applied for adsorptive and/or degradative removal of organic pollutants. In acidic medium, adsorbent became positively charged due to protonation.

Acknowledgment

The authors would like to thank the Department of Mathematics and Statistics, QUEST, Nawab Shah, Pakistan for scientific assistance in developing/designing central composite design and statistical analysis.

References

- [1] G.E.P. Box, K.B. Wilson, On the experimental attainment of optimum conditions, *J. R. Stat. Soc. Ser. B Methodol.*, 13 (1951) 1–45.
- [2] B. Shailendra, S.K. Gupta, D. Apurba, M.K. Jha, V. Bajpai, S. Joshi, A. Gupta, Application of central composite design approach for removal of chromium(VI) from aqueous solution using weakly anionic resin: modeling, optimization, and study of interactive variables, *J. Hazard. Mater.*, 227–228 (2012) 436–444.
- [3] S. Sugashini, S.B.K.M. Meera, Column adsorption studies for the removal of Cr(VI) ions by ethylamine modified chitosan carbonized rice husk composite beads with modelling and optimization, *J. Chem.*, 2013 (2013) 1–11, <https://doi.org/10.1155/2013/460971>.
- [4] A.N. Siyal, S.Q. Memon, M.I. Khaskheli, Optimization and equilibrium studies of Pb(II) removal by *Grewia Asiatica* seed: a factorial design approach, *Pol. J. Chem. Technol.*, 14 (2012) 71–77.
- [5] M.B. Baskan, A. Pala, A statistical experiment design approach for arsenic removal by coagulation process using aluminum sulfate, *Desalination*, 254 (2010) 42–48.
- [6] Z. Javad, S. Ali, R.S. Mohammad, Optimization of Pb(II) biosorption by *Robinia* tree leaves using statistical design of experiments, *Talanta*, 76 (2008) 528–532.
- [7] S.L.C. Ferreira, R.E. Bruns, H.S. Ferreira, G.D. Matos, J.M. David, G.C. Brandão, E.G.P. da Silva, L.A. Portugal, P.S. dos Reis, A.S. Souza, W.N.L. dos Santos, Box–Behnken design: an alternative for the optimization of analytical methods, *Anal. Chim. Acta*, 597 (2007) 179–186.
- [8] M. Iqbal, *Vicia faba* bioassay for environmental toxicity monitoring: a review, *Chemosphere*, 144 (2016) 785–802.
- [9] M. Iqbal, M. Abbas, A. Nazir, Bioassays based on higher plants as excellent dosimeters for ecotoxicity monitoring: a review, *Chem. Int.*, 5 (2019) 1–80.
- [10] M. Abbas, M. Adil, S. Ehtisham-ul-Haque, B. Munir, M. Yameen, A. Ghaffar, G.A. Shar, M.A. Tahir, M. Iqbal, *Vibrio fischeri* bioluminescence inhibition assay for ecotoxicity assessment: a review, *Sci. Total Environ.*, 626 (2018) 1295–1309.
- [11] G. Blázquez, F. Hernáinz, M. Calero, M.A. Martín-Lara, G. Tenorio, The effect of pH on the biosorption of Cr(III) and Cr(VI) with olive stone, *Chem. Eng. J.*, 148 (2009) 473–479.
- [12] M. Akram, H.N. Bhatti, M. Iqbal, S. Noreen, S. Sadaf, Bio-composite efficiency for Cr(VI) adsorption: kinetic, equilibrium and thermodynamics studies, *J. Environ. Chem. Eng.*, 5 (2017) 400–411.
- [13] N. Priyantha, L.B.L. Lim, S. Wickramasooriya, Adsorption behaviour of Cr(VI) by Muthurajawela peat, *Desal. Water Treat.*, 57 (2015) 16592–16600.
- [14] M. Wang, W.Q. Yan, M.L. Chu, T. Li, Z.Y. Liu, Y.Q. Yu, Y.Y. Huang, T.Y. Zhu, M. Wan, C. Mao, D.Q. Shi, Erythrocyte membrane-wrapped magnetic nanotherapeutic agents for reduction and removal of blood Cr(VI), *ACS Appl. Mater. Interfaces*, 12 (2020) 28014–28023.
- [15] G. Bayramoglu, M.Y. Arica, Synthesis of Cr(VI)-imprinted poly(4-vinyl pyridine-co-hydroxyethyl methacrylate) particles: its adsorption propensity to Cr(VI), *J. Hazard. Mater.*, 187 (2011) 213–221.
- [16] Y.A.B. Neolaka, Y. Lawa, J.N. Naat, A.A.P. Riwu, M. Iqbal, H. Darmokoeseoemo, H.S. Kusuma, The adsorption of Cr(VI) from water samples using graphene oxide-magnetic (GO-Fe₃O₄) synthesized from natural cellulose-based graphite (kusambi wood or *Schleichera oleosa*): study of kinetics, isotherms and thermodynamics, *J. Mater. Res. Technol.*, 9 (2020) 6544–6556.
- [17] L.C. Li, Y.L. Xu, D.J. Zhong, Highly efficient adsorption and reduction of Cr(VI) ions by a core-shell Fe₃O₄@UiO-66@PANI composite, *J. Phys. Chem. A*, 124 (2020) 2854–2862.
- [18] M. Barjasteh-Moghaddam, A. Habibi-Yangjeh, Preparation of Cd(OH)₂ nanostructures in water using a simple refluxing method and their photocatalytic activity, *J. Iran Chem. Soc.*, 9 (2012) 163–169.

- [19] F.R. Costa, A. Leuteritz, U. Wagenknecht, D. Jehnichen, L. Häußler, G. Heinrich, Intercalation of Mg–Al layered double hydroxide by anionic surfactants: preparation and characterization, *Appl. Clay Sci.*, 38 (2008) 153–164.
- [20] M.R. Pérez, I. Pavlovic, C. Barriga, J. Cornejo, M.C. Hermosin, M.A. Ulibarri, Uptake of Cu^{2+} , Cd^{2+} and Pb^{2+} on Zn–Al layered double hydroxide intercalated with EDTA, *Appl. Clay Sci.*, 32 (2006) 245–251.
- [21] W.H. Li, A. Liu, H.W. Tian, D.P. Wang, Controlled release of nitrate and molybdate intercalated in Zn–Al-layered double hydroxide nanocontainers towards marine anticorrosion applications, *Colloid Interface Sci. Commun.*, 24 (2018) 18–23.
- [22] L.A. Saghatforoush, S. Sanati, R. Mehdizadeh, M. Hasanzadeh, Solvothermal synthesis of $\text{Cd}(\text{OH})_2$ and CdO nanocrystals and application as a new electrochemical sensor for simultaneous determination of norfloxacin and lomefloxacin, *Superlattices Microstruct.*, 52 (2012) 885–893.
- [23] P.F. Fato, L. Da-Wei, Z. Li-Jun, Q. Kaipei, L. Yi-Tao, Simultaneous removal of multiple heavy metal ions from river water using ultrafine mesoporous magnetite nanoparticles, *ACS Omega*, 4 (2019) 7543–7549.
- [24] S.H. Hasan, P. Srivastava, M. Talat, Biosorption of Pb(II) from water using biomass of *Aeromonas hydrophila*: central composite design for optimization of process variables, *J. Hazard. Mater.*, 168 (2009) 1155–1162.
- [25] I.A. Bhatti, N. Ahmad, N. Iqbal, M. Zahid, M. Iqbal, Chromium adsorption using waste tire and conditions optimization by response surface methodology, *J. Environ. Chem. Eng.*, 5 (2017) 2740–2751.
- [26] D.M. Ruthven, *Principles of Adsorption and Adsorption Processes*, Wiley, New York, 1984.
- [27] S.Q. Memon, S.M. Hasany, M.I. Bhanger, M.Y. Khuhawar, Enrichment of Pb(II) ions using phthalic acid functionalized XAD-16 resin as a sorbent, *J. Colloid Interface Sci.*, 291 (2005) 84–91.
- [28] D. Kundu, S.K. Mondal, T. Banerjee, Development of β -Cyclodextrin-cellulose/hemicellulose-based hydrogels for the removal of Cd(II) and Ni(II): synthesis, kinetics, and adsorption aspects, *J. Chem. Eng. Data*, 64 (2019) 2601–2617.
- [29] N.T.R.N. Kumara, N. Hamdan, M.I. Petra, K.U. Tennakoon, P. Ekanayake, Equilibrium isotherm studies of adsorption of pigments extracted from Kuduk-kuduk (*Melastoma malabathricum* L.) pulp onto TiO_2 nanoparticles, *J. Chem.*, 2014 (2014) 1–6, <https://doi.org/10.1155/2014/468975>.
- [30] M. Yadav, N.K. Singh, Isotherm investigation for the sorption of fluoride onto Bio-F: comparison of linear and non-linear regression method, *Appl. Water Sci.*, 7 (2017) 4793–4800.
- [31] Y.J. Li, B.Y. Gao, T. Wu, D.J. Sun, X. Li, B. Wang, F.J. Lu, Hexavalent chromium removal from aqueous solution by adsorption on aluminum magnesium mixed hydroxide, *Water Res.*, 43 (2009) 3067–3075.
- [32] N.K. Lazaridis, T.A. Pandi, K.A. Matis, Chromium(VI) removal from aqueous solutions by Mg–Al– CO_3 hydrotalcite: sorption–desorption kinetic and equilibrium studies, *Ind. Eng. Chem. Res.*, 43 (2004) 2209–2215.
- [33] C.S. Lei, X.F. Zhu, B.C. Zhu, C.J. Jiang, Y. Le, J.G. Yu, Superb adsorption capacity of hierarchical calcined Ni/Mg/Al layered double hydroxides for Congo red and Cr(VI) ions, *J. Hazard. Mater.*, 321 (2017) 801–811.
- [34] Y. Lu, B. Jiang, L. Fang, F.L. Ling, J.M. Gao, F. Wu, X.H. Zhang, High performance NiFe layered double hydroxide for methyl orange dye and Cr(VI) adsorption, *Chemosphere*, 152 (2016) 415–422.
- [35] H.-P. Chao, Y.-C. Wang, N.T. Hai, Removal of hexavalent chromium from groundwater by Mg/Al-layered double hydroxide s using characteristics of *in-situ* synthesis, *Environ. Pollut.*, 243 (2018) 620–629.
- [36] S.X. Chen, Y.F. Huang, X.X. Han, Z.L. Wu, C. Lai, J. Wang, Q. Deng, Z.L. Zeng, S.G. Deng, Simultaneous and efficient removal of Cr(VI) and methyl orange on LDHs decorated porous carbons, *Chem. Eng. J.*, 352 (2018) 306–315.
- [37] N. Kumar, L. Reddy, V. Parashar, J.C. Ngila, Controlled synthesis of microsheets of ZnAl layered double hydroxides hexagonal layered double hydroxide removal of Cr(VI) ions and anionic dye from water, *J. Environ. Chem. Eng.*, 5 (2017) 1718–1731.
- [38] W.W. Wang, J.B. Zhou, G. Achari, J.G. Yu, W.Q. Cai, Cr(VI) removal from aqueous solutions by hydrothermal synthetic layered double hydroxides: adsorption performance, coexisting anions and regeneration studies, *Colloids Surf., A*, 457 (2014) 33–40.
- [39] F.L. Ling, L. Fang, Y. Lu, J.M. Gao, F. Wu, M. Zhou, B.S. Hu, A novel CoFe layered double hydroxides adsorbent: high adsorption amount for methyl orange dye and fast removal of Cr(VI), *Microporous Mesoporous Mater.*, 234 (2016) 230–238.
- [40] M. Khitous, Z. Salem, D. Halliche, Effect of interlayer anions on chromium removal using Mg–Al layered double hydroxides: kinetic, equilibrium and thermodynamic studies, *Chin. J. Chem. Eng.*, 24 (2016) 433–445.
- [41] T. Kameda, E. Kondo, T. Yoshioka, Treatment of Cr(VI) in aqueous solution by Ni–Al and Co–Al layered double hydroxides: equilibrium and kinetic studies, *J. Water Process Eng.*, 8 (2015) e75–e80.
- [42] N. Jarrar, N.D. Mu'azu, M. Zubair, M. Al-Harathi, Enhanced adsorptive performance of Cr(VI) onto layered double hydroxide-bentonite composite: isotherm, kinetic and thermodynamic studies, *Sep. Sci. Technol.*, 55 (2020) 897–1909.
- [43] X.Y. Yuan, Y.F. Wang, J. Wang, C. Zhou, Q. Tang, X.B. Rao, Calcined graphene/MgAl- layered double hydroxides for enhanced Cr(VI) removal, *Chem. Eng. J.*, 221 (2013) 204–213.
- [44] L. Deng, Z. Shi, L. Wang, S.Q. Zhou, Fabrication of a novel $\text{NiFe}_2\text{O}_4/\text{Zn-Al}$ layered double hydroxide intercalated with EDTA composite and its adsorption behavior for Cr(VI) from aqueous solution, *J. Phys. Chem. Solids*, 104 (2017) 79–90.
- [45] L. Deng, Z. Shi, X.X. Peng, Adsorption of Cr(VI) onto a magnetic $\text{CoFe}_2\text{O}_4/\text{MgAl-LDH}$ composite and mechanism study, *RSC Adv.*, 5 (2015) 49791–49801.
- [46] P. Koilraj, K. Sasaki, Eco-friendly alkali-free arginine-assisted hydrothermal synthesis of different layered double hydroxides and their chromate adsorption/reduction efficiency, *ChemistrySelect*, 2 (2017) 10459–10469.
- [47] K. Zhu, Y. Gao, X.L. Tan, C.L. Chen, Polyaniline-modified Mg/Al layered double hydroxide composites and their application in efficient removal of Cr(VI), *ACS Sustainable Chem. Eng.*, 4 (2016) 4361–4369.